

# Production of biodiesel from waste frying oil using waste calcareous-onyx as unique esterification and transesterification catalytic source

Jorge Cruz-Mérida<sup>a</sup>, Grisel Corro<sup>a,\*</sup>, Fortino Bañuelos<sup>a</sup>, Daniel Montalvo<sup>a</sup>, Umapada Pal<sup>b,\*</sup>

<sup>a</sup> Instituto de Ciencias, Benemérita Universidad Autónoma de Puebla, 4 sur 104, 72000 Puebla, Mexico

<sup>b</sup> Instituto de Física, Benemérita Universidad Autónoma de Puebla, Apdo. Postal J-48, 72570 Puebla, Mexico

## ARTICLE INFO

### Keywords:

Biodiesel  
Calcareous-onyx powder catalyst  
onyx calcination  
Waste frying oil  
Calcite pseudomorph

## ABSTRACT

Biodiesel was produced from waste frying oil (WFO) using waste calcareous-onyx as catalyst. The free fatty acids (FFAs) present in WFO were first esterified with methanol using calcareous-onyx powder calcined at 700 °C (Onyx-700), and the triglycerides transesterification was catalyzed by waste calcareous-onyx powder calcined at 1100 °C (Onyx-1100). Both catalysts were highly active for 5 consecutive reaction runs. DRX and FTIR analyses revealed that Onyx-700 was composed of CaCO<sub>3</sub>, with traces of CaO in calcite pseudomorph, which accelerates methanol adsorption. Onyx-700 prevents reactions between FFAs and CaO, avoiding calcium soap generation. Onyx-1100, which was basically CaO, enhanced triglyceride transesterification process.

## 1. Introduction

To sustain current socio-economic growth, the world has turned towards the generation of energy from renewable sources, not only to reduce environmental pollution but also to make it accessible at affordable cost. Utilization of renewable energy for domestic and industrial purposes can contribute to the depleted fossil fuel reserves, curbing simultaneously the environmental deterioration due to fossil-fuel burning, such as global warming and climate change [1–3]. In this regard, the utilization of biofuels is considered to be a viable alternative to fossil fuels. However, to meet the world's energy demand, the production of biodiesel should be escalated to the industrial level. Moreover, the processes involved in biofuel production must be sustainable and cost-effective.

Biodiesel is a mixture of fatty acid alkyl esters (FAME) and one of the most promising biofuels suitable for substituting fossil fuels in the generation of energy for vehicles and machinery [4]. Biodiesel is a biodegradable, safe-operating biofuel with a low toxic emission profile [5] and is more oxygenated than the conventional diesel. Furthermore, its combustion produces lower emissions of hydrocarbons, SO<sub>x</sub>, particulate matter and fossil carbon dioxide compared with diesel engine exhausts [6].

Biodiesel is produced through the transesterification reaction, a process that converts fats and oils into biodiesel and glycerin (a coproduct). The transesterification process consists of chemical

reactions between triglycerides contained in vegetable oils and alcohol (usually methanol or ethanol) to produce fatty acid alkyl esters and glycerol [7–11]. To accelerate this process, homogeneous catalysts of basic nature, such as NaOH or KOH are preferred [12]. Nevertheless, despite the high yield of biodiesel and short reaction time (30 to 60 min), utilization of these basic catalysts has some serious drawbacks [13,14]. Only the vegetable oils with low free fatty acids and moisture content can be used for the process. While the high-quality edible oils meet this demand, utilizing them in biodiesel production might affect their human consumption adversely [15]. On the other hand, NaOH and KOH cannot be used as catalysts for biodiesel production from waste frying oil or from other non-edible acid oils (e.g., jatropha-curcas oil, pongamia-pinnata oil, etc.), as they present high content of free fatty acids that may lead to oil saponification, thus lowering the yield of the produced biodiesel. Additionally, it is necessary to wash the produced biodiesel with a considerable amount of water to separate the dissolved catalyst, which leads to an increase in the production cost, and consequently an increase in its market price.

To prevent the use of such a large amount of water for removing those homogeneous catalysts from the produced biodiesel, several research groups have utilized CaO as a heterogeneous catalyst for transesterification of triglycerides in edible-grade vegetable oils [16–23]. The sources of CaO utilized for this purpose were limestone and waste seashells, which are abundant and inexpensive materials [11,16–18,20,22,23]. In fact, the utilization of CaO recovered from

\* Corresponding authors.

E-mail addresses: [griselda.corro@correo.buap.mx](mailto:griselda.corro@correo.buap.mx) (G. Corro), [upal@ifuap.buap.mx](mailto:upal@ifuap.buap.mx) (U. Pal).

<https://doi.org/10.1016/j.catcom.2022.106534>

Received 12 July 2022; Received in revised form 10 October 2022; Accepted 14 October 2022

Available online 17 October 2022

1566-7367/© 2022 The Authors. Published by Elsevier B.V. This is an open access article under the CC BY-NC-ND license (<http://creativecommons.org/licenses/by-nc-nd/4.0/>).

limestone and waste seashells for this purpose was expected to bring down the biodiesel production cost. However, this has not been the case, due to the use of expensive edible-grade vegetable oils to perform the process, which hardly produces biodiesel at an affordable cost. On the other hand, waste frying oil (WFO), being a waste and renewable product, is an excellent source for biodiesel production. However, this oil contains a significant number of undesired components such as free fatty acids (FFAs), making the CaO-catalyzed biodiesel production process unviable, unless the FFAs are removed before performing the triglyceride transesterification process.

It is well-known that FFAs react with CaO during triglycerides transesterification process, generating calcium soap, which is a solid mixture of calcium carboxylates. The presence of calcium soap traces brings down the quality of the produced biodiesel. Therefore, utilization of CaO, which is abundant and inexpensive, as an industrial catalyst for biodiesel production from low-quality vegetable oils is hindered by its high reactivity with FFAs present in vegetable oils. Notwithstanding, several efforts have been made to apply CaO as a catalyst for biodiesel production from WFO. In the two-step process utilized for biodiesel production from WFO, the FFAs esterification process was catalyzed by an esterification catalyst such as cation-exchange resins [24]. After this first step, the triglycerides contained in the oil were transesterified using CaO generated from limestone or from other CaO-containing materials [24]. However, as far as our knowledge is concerned, esterification of FFAs has never been performed using Ca compounds such as CaCO<sub>3</sub>.

A preliminary study of the basic properties of natural minerals available in the volcanic region of Puebla city, Mexico, revealed that calcareous-onyx powders are rich in calcium carbonate, with a high density of surface basic sites. On the other hand, it has been shown that while calcium carbonate (CaCO<sub>3</sub>) is not active in the transesterification of triglycerides, it reacts with fatty acids, generating calcium compounds of hydrophobic nature at its surface [25–28]. For example, Osman et al. [25] reported that coating CaCO<sub>3</sub> with stearic acid produces a monolayer of calcium stearate bicarbonate, in which one acid molecule is attached to every surface Ca<sup>2+</sup> ion. The authors also reported that CaCO<sub>3</sub> can be coated with a monolayer of oleic acid which can be polymerized under moderate conditions. On the other hand, through XPS analysis, Frekete et al. [29] suggested the formation of Ca(OH)-(OOCR) during the reaction of CaCO<sub>3</sub> with stearic acid. They also demonstrated that in presence of excess stearic acid, a monolayer is chemisorbed, while other layers are physisorbed in a tail-to-tail arrangement.

Considering these interesting observations, we studied the possibility of esterifying the free fatty acids in WFO with methanol using calcareous-onyx as a catalyst, which is rich in calcium carbonate. The effect of calcination temperature on the performance of calcareous-onyx powder in FFAs esterification with methanol was investigated and correlated with its composition and specific surface basic-sites density.

It is well known that CaCO<sub>3</sub> is transformed into CaO at 850 °C according to reaction 1 [30]:



Therefore, the esterification of FFAs present in WFO was studied using calcareous-onyx powders calcined at temperatures lower than 850 °C to avoid the formation of CaO and its reaction with FFAs, generating calcium soap during the esterification process. Natural calcareous-onyx powder samples were also calcined at higher temperatures (900–1100 °C) for complete oxidation of calcium carbonate to CaO; however, only for their utilization in the transesterification process. The activities of the catalysts were correlated with their physical and physicochemical characteristics determined by XRD, EDS and FTIR spectroscopies, by their specific surface areas and their basic-sites specific densities. The biodiesel process reported in this investigation comprises a first FFAs esterification step, catalyzed by waste onyx powder calcined at  $T < 850$  °C, followed by a triglycerides transesterification second step which is catalyzed by waste calcareous-onyx powder calcined at  $T > 850$  °C.

## 2. Experimental

### 2.1. Waste frying oil (WFO)

WFO was collected from local restaurants of Puebla City, Mexico. The food debris contained in the WFO were removed by filtration, and moisture was eliminated by heating the oil at 120 °C for 2 h. The processed oil was then stored in hermetically sealed PVC cans before its utilization in biodiesel production. The chemical composition of the FFAs present in the processed WFO was analyzed following the certified standard method, NMX-F-017-SCFI-2005. The method consisted in the injection of the sample in the HP5 column of a chromatograph-mass spectrometer HP 6890, provided with a 5973 Network Agilent Technology detector.

### 2.2. Catalytic materials

#### 2.2.1. Preparation

Waste calcareous-onyx powders were collected from the carving sites around Puebla City, Mexico. The collected powders were washed thoroughly with tap-water, dried at 120 °C overnight, and labeled the product as Natural-Onyx. About 100 g of the Natural-Onyx (particle size ranging 0.3–0.5 cm) was calcined under air flow (100 mL/min) at different temperatures from 500 °C to 1100 °C, for 4 h. After cooling down to room temperature, the catalysts were labeled as Onyx-500, Onyx-600, etc., and stored in dry conditions. For comparison, commercial CaCO<sub>3</sub> (Aldrich 99.0%), annealed at different temperatures in similar conditions as that of onyx catalysts for utilizing as references, which were labeled as CaCO<sub>3</sub>-500, CaCO<sub>3</sub>-600, and so on.

#### 2.2.2. Characterization

The calcined calcareous-onyx powders were characterized by X-ray diffraction (XRD) spectroscopy using a Bruker D8 Discover diffractometer with a CuK $\alpha$  radiation ( $\lambda = 1.5406$  Å) source. The diffraction scans were recorded in the 5° - 80° 2 $\theta$  range, with 0.02° per step and a counting time of 0.6 s per point. Fourier-transform infrared (FTIR) spectra of the catalysts were recorded in a Bruker Vertex 70 spectrometer at room temperature in the 4000–800 cm<sup>-1</sup> spectral range with a resolution of 4 cm<sup>-1</sup>. For this study, about 1 mg of each of the catalysts sample was mixed homogeneously with 99 mg of dry KBr powder and compressed to make a pellet of about 5.0 mm diameter.

A Quantachrome Nova-1000 sorptometer was used to measure the N<sub>2</sub> adsorption-desorption isotherms of the onyx catalysts. The BET analysis method was used to estimate the specific surface area (S<sub>g</sub>) of the catalysts based on their N<sub>2</sub> adsorption/desorption isotherms at 77 K. The elemental analysis of the catalysts surfaces was carried out using energy dispersive X-Ray spectroscopy (EDS) technique in a JEOL JSM-7800F field-emission microscope attached with Oxford X-Max analytical attachment.

The surface acid-sites and basic-sites specific densities (number of surface acid or basic sites/g catalyst) of the catalysts were determined according to the process developed and described in a recent work [31]. The described process determines the specific basic- and acid-site densities, by using a pH electrode. In this process, the basic-sites specific density of the samples was estimated by measuring the pOH value of an acetic-acid solution before and after the addition of 1 g of catalyst. The number of basic sites present at the surface of the catalyst was determined by calculating the [OH<sup>-</sup>] from the pOH equilibrium value. Similarly, the acid-site specific density of the samples was determined by measuring the pH value of a NaOH standard solution before and after the addition of 1 g of catalyst. The number of acid sites at the catalyst surface was estimated by calculating the [H<sup>+</sup>] from the pH equilibrium value.

### 2.3. Process for biodiesel production from WFO

The two-step process adapted for biodiesel production was accomplished in a high-pressure, high-temperature reactor of 1 L capacity, which consisted of a stainless-steel reaction vessel provided with a turbine stirrer driven by a high-torque magnetic coupling. The temperature of the reaction mixture was measured with a K-type thermocouple placed inside the vessel. The tightness of the reactor allowed the reactions to be carried out at higher temperatures (60–100 °C) than the boiling point of methanol (64.7 °C). For reaction startup, the WFO, methanol, and the catalyst were loaded into the reaction vessel and mixed at room temperature for 10 min. The stirring speed was fixed at 800 rpm. The first step, i.e. the FFAs esterification process, was conducted by thermal treatment of CH<sub>3</sub>OH and WFO mixture (in 12/1 M ratio), in the presence of Onyx-500, Onyx-600, Onyx-700, Onyx-800, or reference CaCO<sub>3</sub>-700 (0–12 wt% of the used WFO). The second step, i.e. the transesterification of triglycerides, was performed at constant temperature (40–100 °C), utilizing the WFO recovered from the FFAs esterification step and Onyx-900, Onyx-1000, Onyx-1100, or reference CaCO<sub>3</sub>. The chemical reactions occurring during these two steps are presented in Fig. 1.

#### 2.3.1. Preliminary study of the onyx catalysts chemisorption behavior

**2.3.1.1. Estimation of the % FFAs chemisorption on the catalysts surface.** Previous studies have revealed that calcareous-onyx powders are rich in calcium carbonate and free fatty acids (stearic acid, oleic acid) can be chemisorbed on CaCO<sub>3</sub> surface [25–29]. Based on this information, we measured the ability of all the prepared catalysts to chemisorb the free fatty acids present in the WFO. The study was also performed on reference CaCO<sub>3</sub> calcined samples. For that, about 10 g of natural or calcined calcareous-onyx powder catalyst and 100 mL WFO were placed in the reactor and heated under stirring at 100 °C. The mixture was kept under these conditions for 1 h, after which it was cooled to 25 °C. After filtrating the mixture, the amounts of FFAs chemisorbed over the

catalysts were estimated, determining the acid number of the fresh WFO (initial N<sub>acid</sub>) and after its FFAs chemisorption on the catalyst surface process (final N<sub>acid</sub>).

N<sub>acid</sub> was determined according to the ASTM D 664 international standard method. The method allowed us to potentiometrically determine the number of mols of KOH required to neutralize the unknown mols of FFAs present in the WFO and after its FFAs chemisorption on the catalysts surface. The N<sub>acid</sub> numbers were calculated using Eq. (2):

$$N_{acid} = 56.1 \times C \frac{V}{W} \quad (2)$$

where C is the concentration (mols<sup>-1</sup>) of the standard volumetric KOH solution used; V is the volume (mL) of the standard volumetric KOH solution used, W is the mass (g) of the sample; 56.1 is the molecular mass of KOH. The % chemisorption of FFAs (% A<sub>FFAs</sub>) was calculated from the N<sub>acid</sub> values (determined in Eq. (2)), according to Eq. (3):

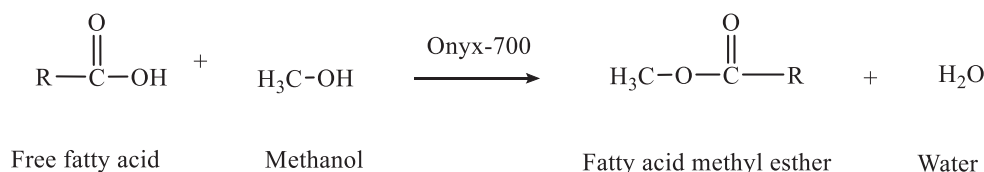
$$A_{FFAs} = \frac{Initial\ N_{acid} - N_{acid\ after\ chemisorption}}{Initial\ N_{acid}} \times 100 \quad (3)$$

where initial N<sub>acid</sub> and N<sub>acid</sub> after chemisorption are the acid numbers measured before and after the FFAs chemisorption process, respectively.

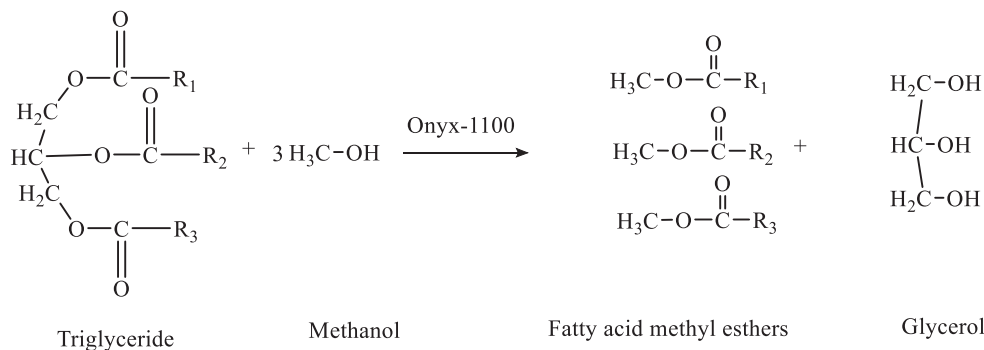
**2.3.1.2. Estimation of CH<sub>3</sub>OH chemisorption on the catalysts surface.** The CH<sub>3</sub>OH chemisorption behavior of natural and calcined calcareous-onyx powder catalysts with methanol was measured. For this purpose, about 10 g of catalyst and 50 mL CH<sub>3</sub>OH were mixed and heated under stirring at 100 °C. After 1 h, the mixture was cooled down to 25 °C. After filtrating the mixture, the pH of the methanol was determined with a glass pH meter.

#### 2.3.2. FFAs esterification with methanol catalyzed by calcined waste onyx powder

Esterification of the FFAs contained in the WFO was performed with methanol (Aldrich, 99%) catalyzed by Natural-Onyx, Onyx-500, Onyx-600, Onyx-700, or Onyx-800 samples. The methanol/WFO molar ratio



Reaction 1: Free fatty acid esterification



Reaction 2: Triglyceride transesterification

Fig. 1. Chemical reactions occurring in the esterification and transesterification steps of biodiesel production.

was maintained at 12/1, which was found to be optimum in our previous studies [31,32]. The catalyst concentration in the reaction mixture was 10 wt% of the used (100 g) WFO. The experiments were performed at a constant temperature in the 40–100 °C range. The reaction was left to proceed for 4 h at a constant stirring speed of 800 rpm. After the desired reaction time, the mixture was cooled to 25 °C and left to separate into two layers; the upper layer consisted of unreacted methanol and the water produced during the esterification process, and the lower layer consisted of methyl esters generated during esterification of FFAs, unreacted triglycerides, and the onyx catalyst (Fig. 1, reaction 1). The lower layer was filtrated to separate the catalyst, and heated at 100 °C to evaporate traces of methanol and water produced during the esterification process. The onyx catalyst was recovered for use in further esterification runs. The study was also performed on the reference CaCO<sub>3</sub>-700 sample. The reactions occurring in this first step are schematically presented in Fig. S-1 (Supplementary Material). The stability and resistance to shattering of the most active catalyst was studied by using it as a catalyst during further consecutive runs without any treatment. The study was performed at the optimal FFAs esterification conditions.

**2.3.2.1. Estimation of acid number and % FFAs esterification.** The acid number  $N_{acid}$  of the fresh WFO and after its FFAs esterification process were estimated according to the ASTM D 664 international standard method (Eq. (2)), as described for the estimation of the % FFAs chemisorption on the catalysts surface. The %-conversion of FFAs (% $C_{FFAs}$ ) was calculated from the  $N_{acid}$  values determined in Eq. (2), according to the following Eq. (4):

$$\%C_{FFAs} = \frac{Initial\ N_{acid} - N_{acid\ after\ esterification}}{Initial\ N_{acid}} \times 100 \quad (4)$$

where (initial  $N_{acid}$ ) and ( $N_{acid}$  after esterification) are the acid numbers measured before and after the FFAs esterification process respectively.

To verify that the decrease of FFAs measured by the potentiometric method is due to FFAs esterification reaction, generating fatty-acids methyl-esters (FAME) (Fig. 1, reaction 1), and not to FFAs adsorption on the catalysts' surfaces, we proceeded to measure the amounts of FAME which may have been generated, according to the EN 14103 test method, described in the following Section 2.3.5.

### 2.3.3. Transesterification of triglycerides with methanol, catalyzed by calcined onyx powder

After drying under stirring conditions, the mixture composed of esterified FFAs and the unreacted triglycerides was transferred to the stainless-steel reactor. A desired amount (0–12 wt% of initial WFO mass) of Onyx-900, Onyx-1000, Onyx-1100 or CaCO<sub>3</sub>-1100, along with six times the stoichiometric amount of methanol, required for the total conversion of the triglycerides in the mixture, were also incorporated. The amount of required methanol was in accordance with our previous optimization results [31–33]. The reactions occurring in this second step are schematically presented in Fig. S-2 (Supplementary Material).

The triglycerides transesterification experiments were performed at constant temperatures in the 40–100 °C range. The catalyst concentration was varied from 0 to 12 wt% of the initial WFO mass. The reaction was left to run for 1 to 6 h. The stirring speed was fixed at 800 rpm. After the desired time of reaction, the reaction mixture was cooled to room temperature and left to settle overnight to separate into two layers. The upper layer was a mixture of the different fatty acid methyl-esters (FAME, biodiesel). The lower layer was a mixture of methanol, glycerol, and the precipitated catalyst that was recovered for the next transesterification cycle. The obtained biodiesel was washed 3 times with hot water (80 °C) and dried under mild stirring at 120 °C for 2 h to eliminate suspended water microdroplets.

To determine the stability and the disaggregation resistance of the onyx catalysts, the recovered samples were used again for further

triglycerides transesterification cycles. The stability study was conducted at the optimal transesterification conditions determined in the present investigation. The catalyst separated from the previous reaction was used for the next run without any treatment or processing.

### 2.3.4. Analysis of produced biodiesel quality

All the tests were performed in triplicate. The content of the produced FAME (biodiesel) was determined through gas chromatography analysis according to the EN 14103 test method. The FAME content (in wt%) was estimated using Eq. (5):

$$FAME\ (wt\%) = \frac{(\sum A_i - A_s)}{A_s} \cdot \frac{C_s \cdot V_s}{m} \times 100 \quad (5)$$

where  $\sum A_i$  is the total peak area of fatty acid methyl esters,  $A_s$  is the area of the internal standard,  $C_s$  is the concentration of the internal standard,  $V_s$  is the volume of the internal standard, and  $m$  is the weight of the sample. The contents of mono-, di-, and triglycerides, and free, bound, and total glycerin in the produced biodiesel were estimated according to the ASTM D 6584 test method using the EZStart chromatography software provided by Shimadzu Co.

### 2.3.5. Analysis of calcium content

The amounts of calcium content in the reaction media and produced biodiesel were evaluated according to the UOP 391-09 test procedure, using a Shimadzu AA-7000 atomic absorption spectrophotometer. The measurements were performed using a hollow Ca cathode lamp, a deuterium background corrector, and an air-acetylene flame. The quantitative evaluations were performed in the integrated absorbance mode at 422.7 nm. The samples were dissolved in a solution of nitric acid before the analysis.

## 3. Results and discussion

### 3.1. Composition analysis of WFO

Quantitative estimation of FFAs present in the used WFO was performed through gas chromatography–mass spectrometry (GC–MS) and results are presented in Table S1. As can be seen in Table S1, the total content of the FFAs in the WFO was about 16.39 wt%.

### 3.2. Catalysts characterization

The specific surface area and pore characteristics of the catalysts are summarized in Table 1. As can be seen, both the specific surface area and average pore size in the onyx catalysts increase with the increase of calcination temperature. Estimated specific densities of acid and basic sites in the onyx catalysts are listed in Table 2. As can be noticed, including the Natural-Onyx powder, all the calcined samples present only basic sites. It can also be seen that the Natural-Onyx, Onyx-500, and Onyx-600 samples present similar values of basic-site specific densities. It is worth noting that CaCO<sub>3</sub> reference sample revealed a comparable basic-site specific density value to those of Natural-Onyx, and of the samples calcined at 500 °C and 600 °C (~10<sup>13</sup>). A further increase in the

**Table 1**  
Catalysts specific surface area and texture characterization.

| Catalyst     | BET specific surface area (m <sup>2</sup> /g) | BET estimated pore volume (cm <sup>3</sup> /g) | BJH pore radius (nm) |
|--------------|---|--|----------------------|
| Natural-Onyx | 0.0019  | 0.0011   | 2.10                 |
| Onyx-600     | 0.11  | 0.0018   | 3.52                 |
| Onyx-700     | 0.55  | 0.0058   | 12.39                |
| Onyx-800     | 0.66  | 0.0072   | 12.39                |
| Onyx-900     | 2.57  | 0.0223   | 1.86                 |
| Onyx-1000    | 2.95  | 0.0238   | 1.76                 |
| Onyx-1100    | 2.44  | 0.0207   | 1.86                 |

**Table 2**  
Estimated basic-site specific density of catalysts.

| Catalyst                | Acid site-specific density (sites/g catalyst) | Basic-site specific density (sites/g catalyst) |
|-------------------------|---|--|
| Natural-Onyx            | 0   | $1.30 \times 10^{13}$                          |
| Onyx-500                | 0   | $2.51 \times 10^{13}$                          |
| Onyx-600                | 0   | $5.01 \times 10^{13}$                          |
| Onyx-700                | 0   | $1.21 \times 10^{20}$                          |
| Onyx-800                | 0   | $3.72 \times 10^{20}$                          |
| Onyx-900                | 0   | $4.37 \times 10^{20}$                          |
| Onyx-1000               | 0   | $5.79 \times 10^{20}$                          |
| Onyx-1100               | 0   | $5.90 \times 10^{20}$                          |
| CaCO <sub>3</sub>       | 0   | $9.79 \times 10^{13}$                          |
| CaCO <sub>3</sub> -700  | 0   | $1.94 \times 10^{20}$                          |
| CaCO <sub>3</sub> -1100 | 0   | $4.30 \times 10^{20}$                          |
| CaO                     | 0   | $3.71 \times 10^{20}$                          |

catalyst calcination temperature increases the basic-site specific density remarkably. The samples calcined at 700–1100 °C presented very high values of the basic-site specific density ( $\sim 10^{20}$ ), comparable to that of CaO.

FTIR spectra of the catalysts recorded at room temperature are presented in Fig. 2. The spectra indicated the presence of CaCO<sub>3</sub> in Natural-Onyx, Onyx-500, Onyx-600, Onyx-700, and Onyx-800. The characteristic absorption IR bands located around 712 cm<sup>-1</sup>, 881 cm<sup>-1</sup>, and the broad IR band appeared in-between 1330 and 1540 cm<sup>-1</sup> with its peak maximum at around 1408 cm<sup>-1</sup> correspond to in-plane bending ( $\nu_4$ ), out-of-plane bending ( $\nu_4$ ), and asymmetric stretching ( $\nu_4$ ) modes of C–O IR bands in the CO<sub>3</sub><sup>2-</sup> group of calcite, respectively [34]. The intensity of these bands decreases as the onyx calcination temperature increases. However, the spectra corresponding to the Onyx-900, Onyx-1000, and Onyx-1100 samples did not reveal those absorption IR bands, indicating the absence of CO<sub>3</sub><sup>2-</sup> group in their structure. However, the FTIR spectra

of these two samples revealed a sharp absorption peak at around 3640 cm<sup>-1</sup>, corresponding to the OH<sup>-</sup> stretching vibration mode, suggesting the presence of Ca(OH)<sub>2</sub>.

Fig. 3 presents the powder XRD patterns of Natural-Onyx and the waste onyx powders calcined at different temperatures. The XRD pattern of Natural-Onyx revealed well-defined diffraction peaks at 27.31, 29.6, 38.49, 41.24, 42.76, 50.29, 52.48, 59.35, 66.02, and 69.07° Bragg angles, which correspond to the (112), (104), (211), (213), (008), (118), (222), (401), (0012), and (410) lattice planes of CaCO<sub>3</sub> in rhombohedral phase (JCPDS no. 01–085-1108). The diffraction peaks appeared around 31.17, 36.25, 43.04, 48.44, 50.29, 56.36, 60.33, 63.33, and 76.81° correspond to the (006), (110), (202), (116), (118), (12–1), (214), (125), and (220) lattice planes of rhombohedral CaCO<sub>3</sub> (JCPDS no. 01–085-1108). Finally, the diffraction peaks appeared around 26.30, 33.20, 37.37, 37.95, 45.92, and 53.08° correspond to the (020), (023), (–311), (–222), (025), and (–315) lattice planes of monoclinic Ca(NO<sub>3</sub>)<sub>2</sub> (JCPDS no. 00–027-0087). However, the diffraction peaks of Ca(NO<sub>3</sub>)<sub>2</sub> were not detected in any of the calcined samples, probably due to the thermal decomposition of calcium nitrate at temperatures  $\geq 500$  °C.

The XRD patterns of the Onyx-500 and Onyx-600 samples revealed the diffraction peaks corresponding to hexagonal CaCO<sub>3</sub> and rhombohedral CaCO<sub>3</sub>, suggesting that during calcination at 500 or 600 °C, this calcium compound remained the same as in Natural-Onyx. It can be noted that the diffraction peaks at 2θ corresponding to CaO or Ca(OH)<sub>2</sub> were not detected in these catalysts.

On the other hand, the XRD patterns of Onyx-900, Onyx-1000 and Onyx-1100 samples (Fig. 3) revealed that the solids were composed of Ca(OH)<sub>2</sub> and CaO. Both the samples revealed diffraction peaks at 18.08, 28.81, 34.19, 47.12, and 50.77° corresponding to the (001), (100), (101), (102), (110) lattice planes of Ca(OH)<sub>2</sub> (JCPDS no. 00–044-1481) along with diffraction peaks around 32.39, 37.52, 53.99, 64.25, 67.45, and 79.78° corresponding to the (111), (200), (220), (311), (222), (400)

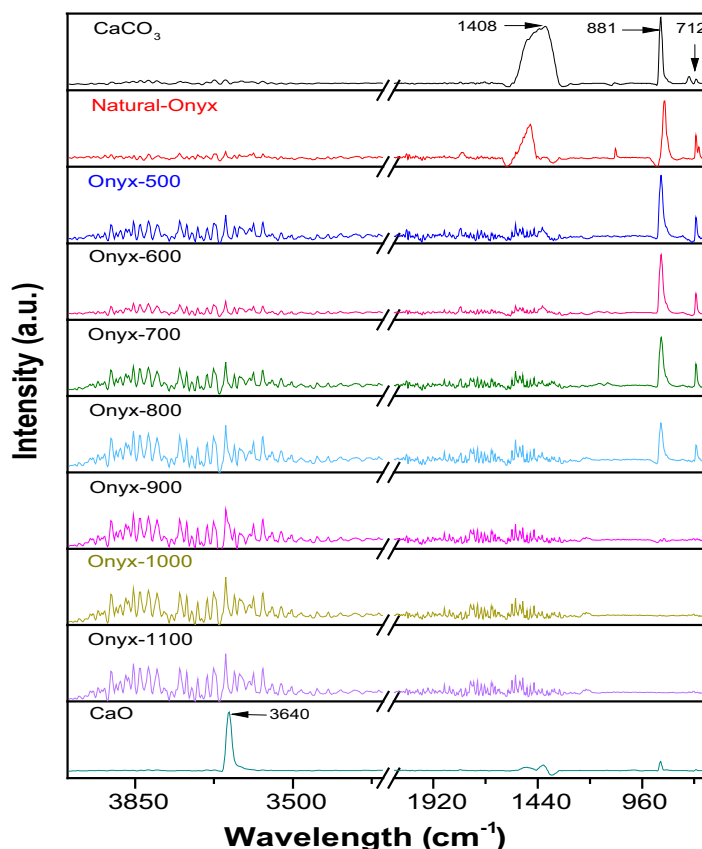


**Fig. 2.** FTIR spectra of waste onyx samples calcinated at different temperatures (600–1100 °C).

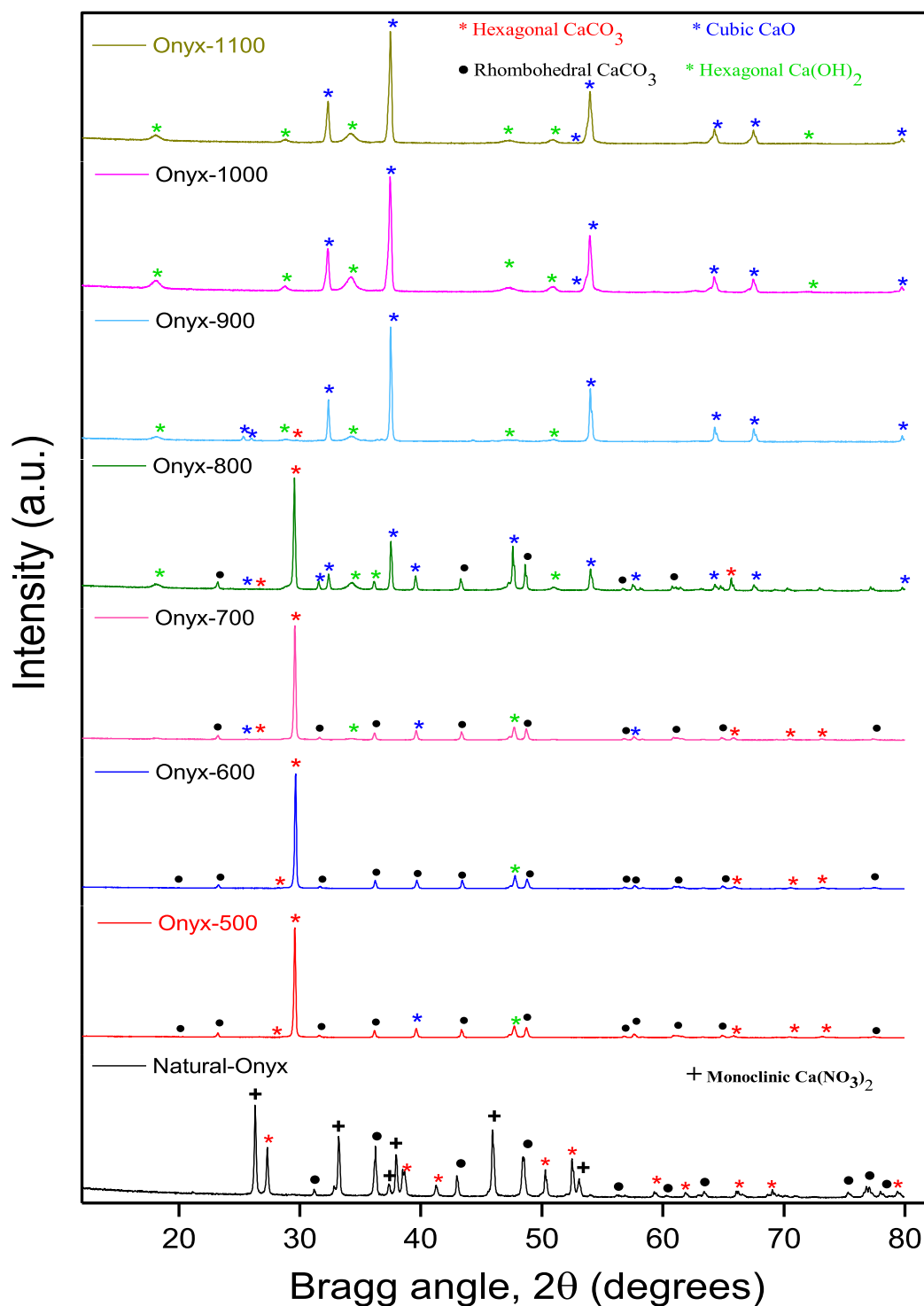


Fig. 3. XRD pattern of onyx powder catalysts annealed at different temperatures.

lattice planes of CaO in cubic phase (JCPDS no. 00-037-1497). None of these catalysts contained  $\text{CaCO}_3$ .

As can be seen in Fig. 3, the XRD pattern of the Onyx-700 sample revealed diffraction peaks mainly of  $\text{CaCO}_3$ , with some weak peaks of CaO and  $\text{Ca(OH)}_2$ , indicating the formation of these compounds in low quantities due to thermal decomposition of calcite. The formation of CaO pseudomorph nanocrystals on the calcination of calcite at 700–750 °C has been observed by Rodríguez-Navarro et al. [35]. In fact, the high specific basic-site density measured for the catalyst (Table 2) is probably due to the formation of CaO and  $\text{Ca(OH)}_2$  at the surface of

$\text{CaCO}_3$  particles. Finally, the XRD pattern of Onyx-800 catalyst is very similar to that of Onyx-700 catalyst; however, with a higher intensity of the peak signals corresponding to CaO and  $\text{Ca(OH)}_2$ . The results indicate that a higher calcination temperature induces a higher degree of conversion of  $\text{CaCO}_3$ , the principal component of the waste calcareous-onyx powder. To compare and better visualize the change in intensity of the principal diffraction peaks, XRD patterns of the Natural-Onyx, Onyx-700 and Onyx 1100 samples are plotted in Fig. S-3 with an amplified intensity scale. It is worth noting the presence of  $\text{Ca(OH)}_2$  in the catalysts annealed at high temperatures (> 800 °C), which indicates that the

formed CaO is partially hydrated. This result can be explained considering that the catalysts were characterized by XRD 2 weeks after their preparation, thus, hydration may have taken place during this time of contact with the ambient air, as has been reported in previous investigations [36,37].

The elemental surface composition of the catalysts estimated by EDS analysis is reported in Table 3.

The EDS analysis revealed that onyx catalysts' surfaces are composed mainly of calcium, carbon and oxygen, as expected. All the calcareous-onyx catalysts presented traces of Na and Sr due to their natural origin. As can be seen in Table 3, the catalysts contain only a very little quantity of Na and Sr, without any other impurity.

### 3.3. Biodiesel production process

#### 3.3.1. Preliminary study of the onyx catalysts chemisorption behavior

The estimated FFAs contents in WFO at the beginning and after 1 h of contact with the calcareous-onyx catalysts (without CH<sub>3</sub>OH) at 100 °C are provided in Table 4. These values indicate that mixing Natural-Onyx, Onyx-500 or Onyx-600 with WFO resulted in a reduction of % FFA content in the liquid phase. The observed reduction is probably due to FFA molecules chemisorption at the catalyst surface [25–29]. The % chemisorption of FFAs values (%A<sub>FFAs</sub>) reported show low amounts of FFAs chemisorbed at the surface of these catalysts. We must recall that these catalysts contain only CaCO<sub>3</sub>. Therefore, the observed values are quite reasonable, as they contain relatively low surface basic-site specific densities (about 10<sup>13</sup> basic-sites/g cat, Table 2).

Mixing WFO with onyx catalysts calcined at higher temperatures (700–1100 °C), which present higher basic-sites specific densities (about 10<sup>20</sup> basic-sites/g cat, Table 2), resulted in a higher % of reduction of FFAs in the WFO. However, the Onyx-900, Onyx-1000, and Onyx-1100 catalysts generated high quantities of calcium soap. The result was expected as these catalysts are composed mainly of CaO (see the XRD and FTIR results presented in Fig. 2 and Fig. S-3). The Onyx-700 and Onyx-800 catalysts did not generate calcium soap in these adsorption conditions, despite their high basic-site specific densities, as will be discussed later.

On the other hand, as shown in Table 4, mixing Natural-Onyx, Onyx-500 or Onyx-600 with only CH<sub>3</sub>OH resulted in an increase of its pH value. The increase of the pH value of methanol was much higher for the mixtures of CH<sub>3</sub>OH with Onyx-700, Onyx-800, Onyx-1000 and Onyx-1100 due to their higher surface basic-site specific density. The increase in pH value can be explained by considering a decrease in methanol molecules in the liquid phase due to the methanol dissociative chemisorption at the basic sites of the catalyst. The increase in pH value could alternatively be due to a dissolved fraction of the catalyst in methanol, generating dissolved calcium species in the liquid phase after contact.

In order to unveil the real reason for the increase in pH value, we determined the Ca species content in methanol, after the experiment (1 h of contact of the catalyst with methanol at 100 °C). Ca content was measured using atomic absorption spectroscopy, as described in Section 2.3.6. The results are reported for Natural-Onyx, Onyx-700 and Onyx-1100 samples in Table S-2 (Supplementary Material). No Ca species were detected in methanol after 1 h of contact with Natural-Onyx or Onyx-700. The result confirms that methanol is effectively chemisorbed

**Table 3**

EDS estimated elemental composition of the pristine and air-annealed calcareous-onyx catalysts.

| Catalyst     | Element (at.%) |       |       |      |      |
|--------------|----------------|-------|-------|------|------|
|              | Ca             | C     | O     | Na   | Sr   |
| Natural-Onyx | 17.21          | 19.54 | 62.91 | 0.24 | 0.35 |
| Onyx-700     | 18.45          | 15.40 | 65.57 | 0.29 | 0.29 |
| Onyx-1100    | 21.12          | 11.31 | 66.21 | 0.74 | 0.62 |

**Table 4**

% FFAs content in WFO and % chemisorption of FFAs (%A<sub>FFAs</sub>) determined after 1 h contact with onyx catalysts at 100 °C. Final pH values of CH<sub>3</sub>OH determined after 1 h contact with onyx catalysts at 100 °C. Initial FFAs content was 16.39% and initial pH of CH<sub>3</sub>OH was 5.68.

| Catalyst                | Final % FFAs content | %A <sub>FFA</sub> | Final pH value of CH <sub>3</sub> OH |
|-------------------------|----------------------|-------------------|--------------------------------------|
| Natural-Onyx            | 15.96                | 2.62              | 7.26                                 |
| Onyx-500                | 15.23                | 7.07              | 7.54                                 |
| Onyx-600                | 15.12                | 7.74              | 7.67                                 |
| Onyx-700                | 9.42                 | 42.52             | 9.97                                 |
| Onyx-800                | 9.55                 | 41.73             | 10.12                                |
| Onyx-900                | 8.19                 | 50.03             | 11.12                                |
| Onyx-1000               | 8.15                 | 50.27             | 11.15                                |
| Onyx-1100               | 8.11                 | 50.51             | 11.26                                |
| CaCO <sub>3</sub>       | 15.52                | 5.30              | 7.39                                 |
| CaCO <sub>3</sub> -700  | 9.32                 | 43.13             | 10.33                                |
| CaCO <sub>3</sub> -1100 | 7.98                 | 51.31             | 11.30                                |
| CaO                     | 8.43                 | 48.56             | 11.00                                |

at the surface of the catalysts, and the catalysts were not dissolved in methanol. However, the analysis revealed the presence of 2.0 ppm of Ca in methanol, after contact with Onyx-1100, indicating that traces of CaO were dissolved in methanol.

Table 4 summarizes the results of chemisorption behavior of the reference CaCO<sub>3</sub>. It can be observed that natural CaCO<sub>3</sub>, CaCO<sub>3</sub>-700 and CaCO<sub>3</sub>-1100 presented similar chemisorption behavior to their onyx-catalysts counterparts, which present natural impurities (Sr, Na) as revealed by EDS. The results suggest that the CH<sub>3</sub>OH and FFAs chemisorption behavior of other CaCO<sub>3</sub>-containing materials (limestone, eggshells, marble, etc.) could be like that of calcareous-onyx catalysts, despite the presence or absence of impurities.

#### 3.3.2. First step - FFAs esterification

As the preliminary studies conducted on the natural and calcined onyx catalysts (Table 4) indicated that FFAs or CH<sub>3</sub>OH can be chemisorbed at the basic sites on the surface of the catalysts, we proceeded to investigate the reaction probability of FFAs esterification with methanol, in the presence of both the FFAs and CH<sub>3</sub>OH in the reaction mixture, considering that both can be adsorbed simultaneously, on the surface of the catalysts.

The results of XRD and FTIR characterization of the catalysts revealed that along with the Natural-Onyx, Onyx-500, Onyx-600, Onyx-700 and Onyx-800 catalysts, these are mainly composed of CaCO<sub>3</sub>, which is an active species, capable of chemisorbing FFAs. Therefore, we determined the %-conversion of FFAs evolution as a function of reaction temperature using only these catalysts. For this study, a fixed methanol/WFO mass ratio (12/1 w/w) and a catalyst/WFO mass ratio (1/10 w/w) were used. These reaction conditions were selected on the basis of the optimal values established in our previous investigations [31,32].

Fig. 4 shows that the FFAs conversion percentages are quite low for the Natural-Onyx, Onyx-500 and Onyx-600 catalysts, as well as for reference CaCO<sub>3</sub> in the studied temperature range. It can also be observed that the blank reaction performed without any catalyst led to a low %FFAs esterification evolution with temperature, corresponding to the non-catalyzed FFAs esterification, which is slightly lower compared with that of these catalysts. The low %-conversion of FFAs can be explained by considering the low basic-site specific densities of the catalysts (Table 2) that might have resulted in the low number of available surface sites for the FFAs and CH<sub>3</sub>OH simultaneous chemisorption (Table 4).

In Fig. 4, it can also be seen that CaCO<sub>3</sub> which presented similar basic-site specific density than Natural-Onyx, Onyx-500 and Onyx-600, revealed a %-conversion of FFAs comparable with these calcareous-onyx catalysts. The Onyx-700 catalyst presented a very high activity for the esterification of FFAs with methanol, attaining 90% FFAs conversion at 100 °C. The high activity presented by this catalyst is due to its high basic-site specific density. It is worth indicating that no calcium soap

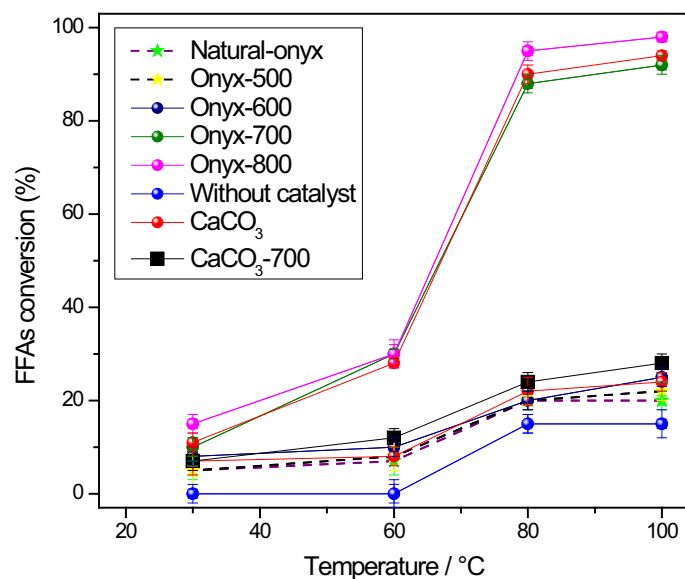


**Fig. 4.** Effect of temperature on FFAs esterification, catalyzed by Natural-Onyx, Onyx-500, Onyx-600, Onyx 700, and, Onyx 800. Reaction conditions: methanol/WFO molar ratio: 12/1 w/w, 4 h.

formation was detected after the reaction. Powder XRD and FTIR analysis of Onyx-700 revealed the presence of low amounts of CaO, which should have reacted with FFAs, generating low amounts of calcium carboxylates (soap). However, this was not the case. The results could be explained by considering that CaO nanocrystals of calcite pseudomorph might have been formed at the surface of CaCO<sub>3</sub> after calcined at 700 °C [35]. However, as these nanocrystals are embedded in CaCO<sub>3</sub> crystallites, only a very few reaction sites (which are principally located at the edges and corners of CaO nanocrystals) are exposed to react with FFAs. Moreover, a fraction of the available reaction sites on the CaO nanocrystal surface is occupied by methanol adsorbed molecules, which reduces the probability of adsorption of FFAs molecules. While using the Onyx-800 catalyst a FFAs conversion of 98% was attained at 100 °C (Fig. 4), but calcium soap was formed during the reaction. In fact, the formation of calcium soap started even at 60 °C for this catalyst. The formation of calcium soap even at such low reaction temperature is ascribed to the presence of CaO in the catalyst in high concentrations [11,24]. It can be observed (Fig. 4) that natural CaCO<sub>3</sub> and CaCO<sub>3</sub>-700 presented similar FFAs esterification to their onyx-catalysts counterparts.

To evaluate the possible solubilization of the Onyx-700 catalyst in the reaction medium, which might have generated a homogeneously catalyzed FFAs esterification contribution, we performed the following catalyst solubility test. Using the same FFAs esterification conditions, we determined the FFAs %-conversion evolution at 60 °C. At this reaction temperature, a 30% conversion of FFAs was attained. The reactor was then cooled to room temperature, to separate by filtration the catalyst from the liquid reaction mixture, and restarted the reaction conditions with the liquid medium only. The FFAs %-conversion was then measured at 80 and 100 °C. As can be seen in Fig. S-4 (Supplementary Material), the FFAs %-conversion only increased from 30% FFAs conversion at 60 °C to about 45% at 100 °C. This slight increase might be due to the non-catalyzed (without catalyst) FFAs conversion, which evolves with temperature as shown in Fig. S-4. The catalyzed FFAs esterification stopped when Onyx-700 was removed from the reaction medium, indicating that the catalyst was not dissolved in the liquid phase of the reactant mixture. Therefore, there was no homogeneously catalyzed FFAs esterification contribution.

The results obtained from the FFAs esterification with methanol using Onyx-800 catalyst and the preliminary tests of all the catalysts performed earlier, suggest that the Onyx-900, Onyx-1000 and Onyx-

1100 catalysts are not effective for FFAs esterification process as they contain CaO in a high concentration, which reacts with FFAs to produce calcium carboxylates. For this reason, those catalysts were not utilized for the FFAs esterification process. Instead, we utilized the Onyx-700 catalyst which does not produce calcium soap reacting with FFAs in the WFO.

### 3.3.3. Stability tests for the Onyx-700 catalyst

To test the stability of the Onyx-700 catalyst in FFAs esterification process, the reaction was repeated for 7 consecutive times using the as-recovered catalyst without any washing process, under the optimized reaction conditions determined in this investigation e.g. methanol/WFO mass ratio (12/1 w/w), catalyst/WFO mass ratio (1/10 w/w), reaction temperature (100 °C), and reaction time of 4 h. As can be noticed in Table S-3 (Supplementary Material), for the first 5 reaction runs, the FFAs esterification activity of the catalyst decreased slightly. Nevertheless, after the 5th reaction run, the FFAs %-conversion decrease was higher.

To unveil the cause of the decrease in FFAs esterification performance of Onyx-700 with successive reaction runs, after the 7th run the catalyst was recovered by filtration and characterized by its basic-site specific density (as described in Section 2.2) without any treatment. The value measured for the final basic-site specific density of the used Onyx-700 was  $1.07 \times 10^{20}$ , which is slightly lower than that of the fresh Onyx-700 ( $1.21 \times 10^{20}$ ), as shown in Table 2. The basic-site specific density remained almost same, suggesting that the decrease in FFAs esterification activity of Onyx-700 cannot be due to a change in the basic properties of the catalyst.

In Table S-3, it can be observed that after the first run, the 90% FFAs conversion was attained. The 10% FFAs molecules might have remained on CaCO<sub>3</sub> surface sites, and could have been polymerized under these conditions, as was reported by Osman et al. [25] in a study of coating CaCO<sub>3</sub> with stearic acid. The number of occupied CaCO<sub>3</sub> surface sites may have increased during the following reaction runs, thus the polymerized FFAs may also have increased, masking the catalytic surface sites and preventing further adsorption of reactants, while keeping unaltered the basic-site specific density.

To demonstrate that the FFAs conversion values determined using Eq. (4) do not correspond to FFAs chemisorption on the catalyst surface, but to the FFA esterification reaction, which produces fatty-acids methyl-ester, the amounts of fatty-acids methyl-esters generated

during the reaction were measured (Fig. 1, reaction 1). Fig. S-5 (Supplementary Material) shows the FAME percentage evolution measured as a function of the FFAs %-conversion at different esterification temperatures. It can be observed a linear dependence of generated FAME with FFAs %-conversion during the reaction. This result shows that the FFA esterification catalyzed by Onyx-700 takes place effectively.

### 3.3.4. Second step: transesterification of triglycerides catalyzed by Onyx-900, Onyx-1000 and Onyx-1100

Once the FFAs of the WFO are converted to fatty acid methyl-esters, the triglycerides transesterification reaction was performed to produce corresponding fatty acid methyl-esters (Fig. 1, reaction 2) using CaO-rich calcinated waste onyx catalysts. For this purpose, the dried WFO recovered after FFAs esterification catalyzed by Onyx-700 was transferred to the stainless-steel reactor with either Onyx-900, Onyx-1000, Onyx-1100 or reference  $\text{CaCO}_3$ -1100 catalyst. The transesterification reaction conditions were optimized as described below.

First, we examined the evolution of FAME (in wt%) as a function of reaction temperature estimated using Eq. (4). For the study, a fixed methanol/WFO molar ratio of 6/1 and a catalyst/WFO mass ratio (1/10 w/w) were used. These reaction conditions were selected considering the optimal values established in our previous investigations [31,32].

Fig. 5 shows the evolution of FAME (wt%) as a function of reaction temperature for different catalysts. As can be seen, the three catalysts present very similar FAME evolution. The activity of all the three catalysts is high at  $T \geq 70$  °C. It can be observed that reference  $\text{CaCO}_3$ -1100 presented a slightly lower triglycerides transesterification activity behavior than those of Onyx-900, Onyx-1000 and Onyx-1100.

Reaction time affects strongly the FAME evolution rate. A longer reaction time increases the probability that the triglyceride molecules reach the active sites at the catalyst surface. Fig. 6 shows the effect of reaction time on the FAME evolution in the reactions catalyzed by the Onyx-900, Onyx-1000, Onyx-1100 or reference  $\text{CaCO}_3$ -1100 catalyst. It can be seen that under the reaction conditions used (100 °C reaction temperature, methanol/WFO molar ratio 6/1, and catalyst/WFO mass ratio 1/10), the FAME evolution increases with reaction time up to 4 h, reaching to about 96%. After 5 h of reaction, only a slight increase in % FAME was measured.

The effects of catalyst content (wt%) on FAME evolution (wt%) are presented in Fig. 7. The catalyst/WFO mass ratio was varied from 4 to 12%. All the catalysts presented similar behavior under the used (fixed)

reaction conditions (reaction temperature: 100 °C, methanol/WFO molar ratio: 6/1, and reaction time: 4 h). The rate of FAME evolution increased with the increase of catalyst loading. The FAME evolution reached its maximum for about 10 wt% of catalyst loading, which remained almost constant for further increase of the catalyst mass.

The results presented in Figs. 5-7 indicate that Onyx-900, Onyx-1000 and Onyx-1100 present high FAME production yield, and can be used in biodiesel production from WFO after its FFAs esterification catalyzed by Onyx-700.

### 3.3.5. Stability of Onyx-900, Onyx-1000, and Onyx-1100 catalysts

To examine the reusability and operational stability of the prepared Onyx-900, Onyx-1000 and Onyx-1100 catalysts, these were recovered by filtrating the reaction mixtures after the completion of the first transesterification run. Consequently, the recovered catalysts were utilized in the next transesterification runs under the same reaction conditions as of the first run. Fig. 8 shows the FAME evolution performance of the catalysts in the consecutive transesterification runs. As can be noticed, none of these catalysts deactivated significantly until the 5th reaction run. Onyx-900 and Onyx-1000 shattered strongly after the 5th and 6th run, respectively. Onyx-1100 remained highly active for the reaction until the 7th run and was easily separated from the liquid reaction mixture. Reference  $\text{CaCO}_3$ -1100 deactivated during the 1st run and shattered strongly during the 2nd run.

The cause of the decrease in triglycerides transesterification performance of Onyx-1100 with successive reaction runs was investigated in the following way. After the 7th run, the catalyst was recovered by filtration and characterized for its basic-site specific density (as described in Section 2.2) without any treatment. The value estimated for the final basic-site specific density of the used Onyx-1100 was slightly lower ( $4.20 \times 10^{20}$ ) than that of the fresh Onyx-1100 ( $5.90 \times 10^{20}$ , Table 2). This gradual catalyst deactivation cannot be explained by its slight decrease in basic-site specific density. A possible explanation of the decrease in activity of the catalyst could be the gradual catalyst mass loss during the successive triglycerides transesterification runs. The catalyst mass loss could be due, on one hand, to CaO leaching during the reaction under vigorous magnetic stirring, in which catalyst micro-crystallites would be dispersed onto the liquid reaction medium. On the other hand, during the triglycerides transesterification reaction, glycerol is generated as a byproduct (Fig. 1, reaction 2). It has been reported that glycerol can react with CaO generating calcium

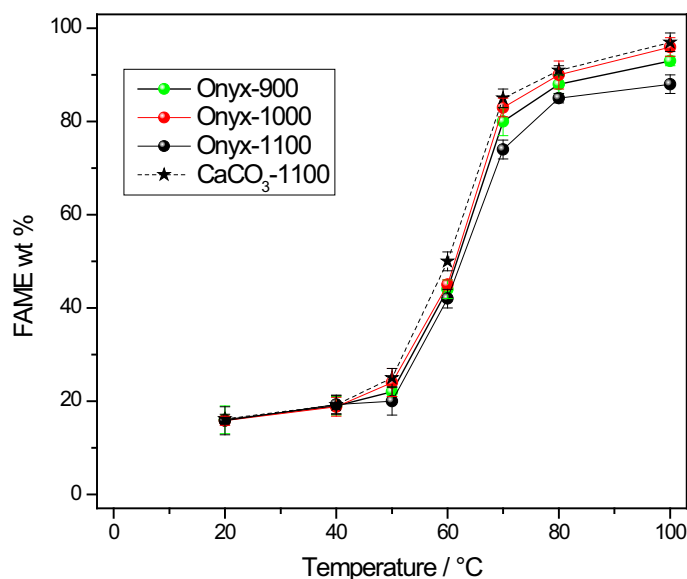


Fig. 5. Effect of temperature on FAME evolution catalyzed by Onyx-900, Onyx-1000, Onyx-1100 or reference  $\text{CaCO}_3$ -1100. Reaction conditions: methanol/WFO molar ratio: 6/1, catalyst/WFO mass ratio: 1/10, reaction time: 4 h.

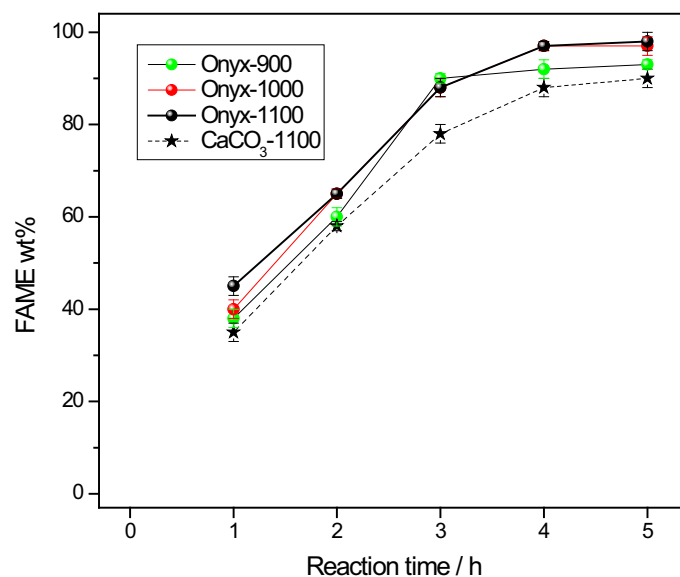


Fig. 6. Effect of reaction time on FAME evolution catalyzed by Onyx-900, Onyx-1000, Onyx-1100 or reference CaCO<sub>3</sub>-1100. Reaction conditions: methanol/WFO molar ratio: 6/1, catalyst/WFO mass ratio: 1/10, reaction temperature: 100 °C.

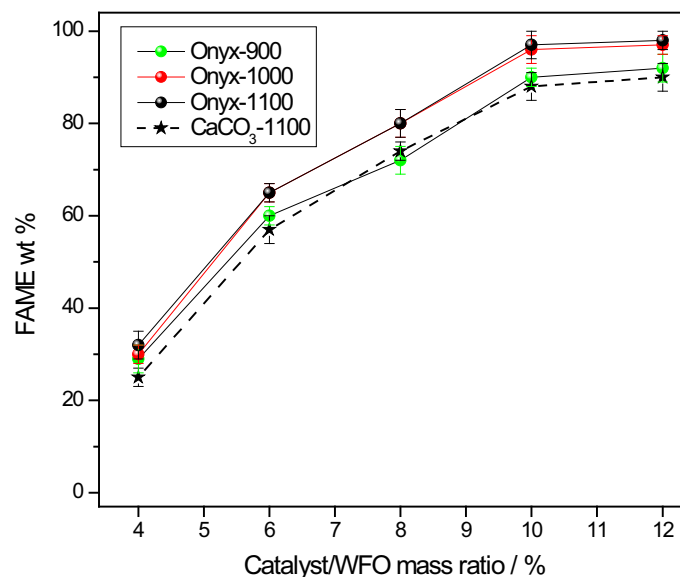


Fig. 7. Effect of catalyst/WFO mass ratio on FAME evolution catalyzed by Onyx-900, Onyx-1000, Onyx-1100 or reference CaCO<sub>3</sub>-1100. Reaction conditions: methanol/WFO molar ratio: 6/1, reaction time: 4 h; reaction temperature: 100 °C.

diglyceroxide, which is soluble in methanol [38]. Calcium diglyceroxide would be produced to the detriment of the catalyst, reducing its initial mass, and reducing the triglycerides transesterification reaction to produce FAME.

On the other hand, based on Tables 2 and 4, and Figs. 4-7, it can be concluded that the commercial CaCO<sub>3</sub>, CaCO<sub>3</sub>-700 and CaCO<sub>3</sub>-1100 catalysts, which are reasonably high purity materials, presented similar FFAs esterification and triglycerides transesterification catalytic behaviors to that of their calcareous-onyx counterparts, which contain impurities such as Na and Sr. The results indicate that other abundant and inexpensive waste materials such as waste seashells and marble, which are mainly composed of CaCO<sub>3</sub>, can be thermally treated to generate useful catalysts, capable of producing biodiesel from WFO, although they probably contain impurities.

### 3.3.6. Efficiency performance

In the optimized conditions of FAME evolution reaction, only about 14 wt% FAME conversion occurred in the reaction performed without any catalyst. This value was considered as the conversion reference (% C<sub>Ref</sub>) to estimate the catalytic efficiency of the onyx catalysts for the transesterification reaction. The catalytic efficiency of the catalysts was calculated using the following Eq. (6):

$$\text{Catalyst efficiency} = \frac{\%C_{\text{Cat}} - \%C_{\text{Ref}}}{100 - \%C_{\text{Ref}}} \quad (6)$$

where %C<sub>Cat</sub> is the triglycerides %-conversion measured for each catalyst. The calculated values of efficiency for the three catalysts are presented in Table S-4 (Supplementary Material). These results indicate that while Onyx-900 and Onyx-1000 resisted only 5 and 6 reaction runs, respectively, due to shattering, Onyx-1100 resisted 7 reaction runs thus presenting a high efficiency for the reaction.

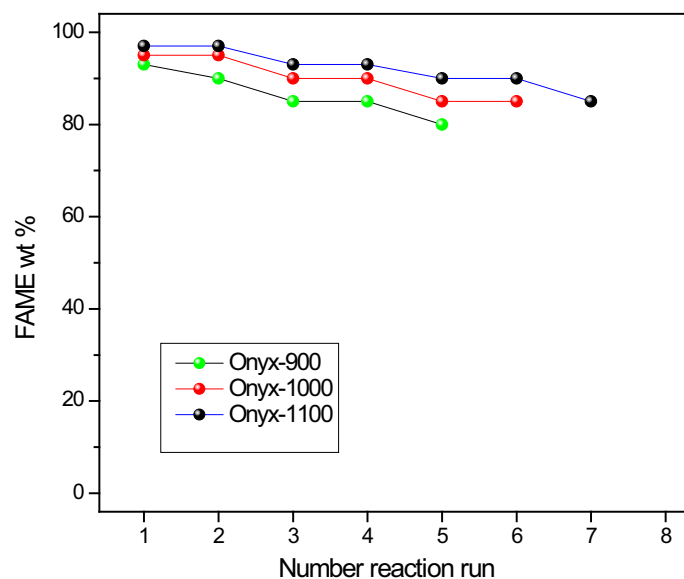


**Fig. 8.** Evolution of FAME at different runs for the Onyx-900, Onyx-1000 or Onyx-1100 catalysts. Reaction conditions: methanol/WFO molar ratio: 6/1, catalyst/WFO mass ratio: 1/10, reaction time: 4 h; reaction temperature: 100 °C.

### 3.3.7. Biodiesel characterization

The characteristics of the obtained biodiesel and its composition for the 1st and 7th runs are provided in Table 5. The contents of mono, di, and triglycerides, as well as free, bound and total glycerin in the produced biodiesel determined by the ASTM D 6584 test are very low. The (Ca + Na) content in the produced biodiesel is a bit higher than the prescribed range, which might hinder its use as a fuel. However, the (Ca + Na) content, which is mainly Ca, obtained during the 1st and 7th runs, is probably due to CaO leaching from onyx-catalysts. The CaO leached in the reaction medium may homogeneously catalyze the transesterification reaction of triglycerides. Although the Ca content range detected in the produced biodiesel is in-between 15 and 25 ppm, the contribution of homogeneous reaction catalyzed by the leached CaO should indeed be very small. The results are in good agreement with the previous investigations on triglyceride methanolysis using CaO. The

**Table 5**

Characteristics of the biodiesel obtained from WFO using Onyx-700 for catalyzing FFAs esterification and Onyx-1100 for catalyzing triglyceride transesterification.

| Characteristics/properties             | Estimated values                     |                                      | Allowed values                             |
|--|--------------------------------------|--------------------------------------|--|
|  | 1st run                              | 7th run                              |  |
| Density at 15 °C                       | 880 kg •m <sup>-3</sup>              | 885 kg •m <sup>-3</sup>              | (860–900) kg •m <sup>-3</sup>              |
| Kinematic viscosity at 40 °C           | 4.1 mm <sup>2</sup> •s <sup>-1</sup> | 4.8 mm <sup>2</sup> •s <sup>-1</sup> | (3.5–5.0) mm <sup>2</sup> •s <sup>-1</sup> |
| Acid number                            | 0.34 mg KOH•g <sup>-1</sup>          | 0.34 mg KOH•g <sup>-1</sup>          | (0.0–0.5) mg•g <sup>-1</sup>               |
| Ester content                          | 96.2 wt%                             | 85.0 wt%                             | (96.5–100) wt%                             |
| Esters with >4 double bonds            | 0.0% wt%                             | 0.0% wt%                             | (0.0–1.0) wt%                              |
| Ester content after methanol washing   | 98.3 wt%                             | 94.5 wt%                             | (96.5–100) wt%                             |
| Esters from linolenic acid             | 0.01 wt%                             | 0.95 wt%                             | (0.0–12.0) wt%                             |
| Monoglyceride                          | 0.40 wt%                             | 0.74 wt%                             | (0.0–0.8) wt%                              |
| Diglyceride                            | 0.25 wt%                             | 0.25 wt%                             | (0.0–0.2) wt%                              |
| Triglyceride                           | 0.00 wt%                             | 0.25 wt%                             | (0.0–0.2) wt%                              |
| Free glycerin                          | 0.01 wt%                             | 0.01 wt%                             | (0.0–0.02) wt%                             |
| Bound glycerin                         | 0.20 wt%                             | 0.20 wt%                             | (0.0–0.23) wt%                             |
| Total glycerin                         | 0.21 wt%                             | 0.21 wt%                             | (0.0–0.25) wt%                             |
| Ca + Na content                        | 15 mg•kg <sup>-1</sup>               | 25 mg•kg <sup>-1</sup>               | (0.0–5.0) mg•kg <sup>-1</sup>              |
| Ca + Na content after methanol washing | 3.0 mg•kg <sup>-1</sup>              | 5.0 mg•kg <sup>-1</sup>              | (0.0–5.0) mg•kg <sup>-1</sup>              |

results reported in this investigation showed that the homogeneous contribution arising from CaO leached species can be considered negligible [38].

On the other hand, as discussed in Section 3.3.5, glycerol produced in the transesterification process might have reacted with the catalyst (CaO) surface, producing Ca-diglyceroxide [38], which is soluble in methanol but has not been removed fully during the water-washing process of the produced biodiesel. To verify this assumption, we performed an additional test by mixing the produced biodiesel with methanol (in 2:1 vol/vol) to dissolve the possible remaining Ca-diglyceroxide compound under vigorous magnetic stirring for 10 min at room temperature. The separated biodiesel from the mixture was dried at 120 °C and analyzed by atomic absorption spectroscopy. The (Ca + Na) concentrations determined in the methanol-washed biodiesel produced in the 1st and 7th cycles were reduced to 3 ppm and 5 ppm, respectively. Interestingly, washing of biodiesel with methanol at the same time, resulted in an increase in the ester content to 98.3 wt% and 94.5 wt% for the 1st and 7th run, respectively, as can be observed in Table 5. Therefore, the biodiesel obtained through the process proposed in this work has all the characteristics within the prescribed limits of international standards.

The biodiesel obtained by the process proposed in this study meets the demands of the international requirements for its use and commercialization. WFO used as feedstock is a renewable waste, therefore, its use for biodiesel production prevents the additional fossil CO<sub>2</sub> emissions from unavoidable oil seeds cultivation [39]. Calcareous-onyx is an inexpensive and abundant waste, whose thermic process for catalyst preparation could increase the CO<sub>2</sub> emissions and the biofuel carbon footprint, if the electricity used for heating is not obtained by renewable energy generators, such as solar heat concentrators. The characteristics of this biodiesel production process suggest that it can be applied at the industrial level, at low cost and high conversion efficiency, which are the major obstacles that impede industrial production of enzymatic biodiesel [40].

## 4. Conclusions

We have demonstrated the utilization of calcareous-onyx powder, a waste material of architectural and artistic works, as low-cost esterification and transesterification catalyst for producing biodiesel from WFO. The two-steps process adopted for biodiesel production in this

work demonstrated that it is possible to use waste onyx, or other waste materials containing  $\text{CaCO}_3$  for biodiesel production using non-edible oils containing high contents of FFAs. The FFAs esterification and triglycerides transesterification activities of the waste calcareous-onyx catalyst can be tuned by controlling its calcination temperature. The waste calcareous-onyx powder calcined at  $700^\circ\text{C}$  was found to be a very active catalyst for esterification of FFAs in WFO. On the other hand, the waste calcareous-onyx powder calcined at  $1100^\circ\text{C}$  performed as an excellent catalyst for transesterification of triglycerides. The biodiesel production process presented in this work can open up a viable possibility for producing high quality biodiesel from WFO at industrial level in economic way.

## Declaration of Competing Interest

We declare no competing interests.

## Data availability

No data was used for the research described in the article.

## Acknowledgements

The authors acknowledge the Vicerrectoría de Investigación y Estudios de Posgrado (VIEP), BUAP (Project Grant # 2022), Secretaría de Energía (SENER) and Consejo Nacional de Ciencia y Tecnología (CONACYT), Mexico (Project Grants # 250014 & CB-A1-S-26720) for their financial supports.

## Appendix A. Supplementary data

Supplementary data to this article can be found online at <https://doi.org/10.1016/j.catcom.2022.106534>.

## References

- I.B. Banković-Ilić, M.R. Miladinović, O.S. Stamenković, V.B. Veljković, Application of nano  $\text{CaO}$ -based catalysts in biodiesel synthesis, *R. Sustain. Energy Rev.* 72 (2017) 746–760, <https://doi.org/10.1016/j.rser.2017.01.076>.
- X.X. Yang, Y.T. Wang, Y.T. Yang, E.Z. Feng, J. Luo, F. Zhang, W.J. Yang, G.R. Bao, Catalytic transesterification to biodiesel at room temperature over several solid bases, *E. Convers. Manage.* 164 (2018) 112–121, <https://doi.org/10.1016/j.enconman.2018.02.085>.
- A.I. Osman, M. Hefny, M.I.A. Abdel Maksoud, A.M. Elgarahy, D.W. Rooney, Recent advances in carbon capture storage and utilization technologies: a review, *E. Chem. Lett.* 19 (2021) 797–849, <https://doi.org/10.1007/s10311-020-01133-3>.
- R.U. Owolabi, A.L. Adejumo, A.F. Aderibigbe, Biodiesel: fuel for the future (a brief review), *Int. J. Energy Eng.* 2 (2012) 223–231, <https://doi.org/10.5923/j.ijee.20120205.06>.
- Y. Liu, P. Zhang, M. Fan, P. Jiang, Biodiesel production from soybean oil catalyzed by magnetic nanoparticle  $\text{MgFe}_2\text{O}_4/\text{CaO}$ , *Fuel.* 164 (2016) 314–321, <https://doi.org/10.1016/j.fuel.2015.10.008>.
- Z. Wen, X. Yu, S.T. Tu, J. Yan, E. Dahlquist, Synthesis of biodiesel from vegetable oil with methanol catalyzed by Li-doped magnesium oxide catalysts, *Appl. Energy* 87 (2010) 743–748, <https://doi.org/10.1016/j.apenergy.2009.09.013>.
- Y.C. Sharma, B. Singh, An ideal feedstock, kusun (*Schleichera triguga*) for preparation of biodiesel: optimization of parameters, *Fuel.* 89 (2010) 1470–1474, <https://doi.org/10.1016/j.fuel.2009.10.013>.
- J. Xue, T.E. Grift, A.C. Hansen, Effect of biodiesel on engine performances and emissions, *R. Sustain. Energy Rev.* 15 (2011) 1098–1116, <https://doi.org/10.1016/j.rser.2010.11.016>.
- K. Narasimharao, D.R. Brown, A.F. Lee, A.D. Newman, P.F. Siril, S.J. Tavener, K. Wilson structure-activity relations in Cs-doped heteropolyacid catalysts for biodiesel production, *J. Catal.* 248 (2007) 226–234, <https://doi.org/10.1016/j.jcat.2007.02.016>.
- B.M.E. Russbueldt, W.F. Hoelderich, New rare earth oxide catalysts for the transesterification of triglycerides with methanol resulting in biodiesel and pure glycerol, *J. Catal.* 271 (2010) 290–304, <https://doi.org/10.1016/j.jcat.2010.02.005>.
- M. López-Granados, A.C. Alba-Rubio, F. Vila, D.M. Alonso, R. Mariscal, Surface chemical promotion of calcium oxide catalysts in biodiesel production reaction by the addition of monoglycerides, diglycerides and glycerol, *J. Catal.* 276 (2010) 229–236, <https://doi.org/10.1016/j.jcat.2010.09.016>.
- B. Smith, H.C. Greenwell, A. Whiting, Catalytic upgrading of tri-glycerides and fatty acids to transport biofuels, *Energy Environ. Sci.* 2 (2009) 262–271, <https://doi.org/10.1039/B814123A>.
- A.P. Vyas, J.L. Verma, N. Subrahmanyam, A review on FAME production processes, *Fuel.* 89 (2010) 1–9, <https://doi.org/10.1016/j.fuel.2009.08.014>.
- M.P. Dorado, E. Ballesteros, F.J. López, M. Mittelbach, Optimization of alkali-catalyzed transesterification of brassica Carinata oil for biodiesel production, *Energy Fuel* 18 (2004) 77–83, <https://doi.org/10.1021/ef0340110>.
- R. Foroutan, H. Esmaili, S.M. Mousavi, S.A. Hashemi, G. Yeganeh, The physical properties of biodiesel-diesel fuel produced via transesterification process from different oil sources, *Quant. Struct. Activity Relation.* 6 (2019) 415–424, <https://doi.org/10.22036/PCR.2019.173224.1600>.
- N. Mansir, S.H. Teo, U. Rashid, M.I. Saiman, Y.P. Tan, G.A. Alsultan, Y.M. Taufiq-Yap, Modified waste egg shell derived bifunctional catalyst for biodiesel production from high FFA waste cooking oil. A review, *R. Sustain. Energy Rev.* 82 (2018) 3645–3655, <https://doi.org/10.1016/j.rser.2017.10.098>.
- A. Laca, M. Díaz, Eggshell waste as catalyst: a review, *J. Environ. Manage.* 197 (2017) 351–359, <https://doi.org/10.1016/j.jenvman.2017.03.088>.
- A. Kawashima, K. Matsubara, K. Honda, Acceleration of catalytic activity of calcium oxide for biodiesel production, *Bioresour. Technol.* 100 (2009) 696–700, <https://doi.org/10.1016/j.biortech.2008.06.049>.
- D.Y.C. Leung, X. Wu, M.K.H. Leung, A review on biodiesel production using catalyzed transesterification, *Appl. Energy* 87 (2010) 1083–1095, <https://doi.org/10.1016/j.apenergy.2009.10.006>.
- T.A. Degfie, T.T. Mamo, Y.S. Mekonnen, Optimized biodiesel production from waste cooking oil (WCO) using calcium oxide ( $\text{CaO}$ ) Nano-catalyst, *Sci. Report.* 9 (2019) 18982, <https://doi.org/10.1038/s41598-019-55403-4>.
- T.T. Mamo, Y.S. Mekonnen, Microwave-assisted biodiesel production from microalgae, *scenedesmus* species, using goat bone-made nano-catalyst, *Appl. Biochem. Biotechnol.* 190 (2020) 1147–1162, <https://doi.org/10.1007/s12010-019-03149-0>.
- N. Tshizanga, E.F. Aransiola, O. Oyekola, Optimisation of biodiesel production from waste vegetable oil and eggshell ash, *S. Afr. J. Chem. Eng.* 23 (2017) 145–156, <https://doi.org/10.1016/j.sajce.2017.05.003>.
- P. Verma, M.P. Sharma, Review of process parameters for biodiesel production from different feedstocks, *R. Sustain. Energy Rev.* 62 (2016) 1063–1071, <https://doi.org/10.1016/j.rser.2016.04.054>.
- M. Kouzu, T. Kasuno, M. Tajika, Y. Sugimoto, S. Yamanaka, J. Hidaka, Calcium oxide as a solid base catalyst for transesterification of soybean oil and its application to biodiesel production, *Fuel.* 87 (2008) 2798–2806, <https://doi.org/10.1016/j.fuel.2007.10.019>.
- M.A. Osman, U.W. Suter, Surface treatment of calcite with fatty acids; structure and properties of the organic monolayer, *Chem. Mater.* 14 (2002) 4408–4415, <https://doi.org/10.1021/cm021222u>.
- A.W. Jeon, S. Park, J.H. Bang, S. Chae, K. Song, Non polar surface modification using fatty acids and its effect on calcite from mineral carbonation of desulfurized gypsum, *Coatings* 8 (1) (2017) 43, <https://doi.org/10.3390/coatings8010043>.
- B. Röcker, G. Mäder, F.W. Monnard, M. Jancikova, M. Welker, J. Schoelkopf, S. Yildirim, Evaluation of the potential of modified calcium carbonate as a carrier for unsaturated fatty acids in oxygen scavenging applications, *Materials.* 14 (2021) 500, <https://doi.org/10.3390/ma14175000>.
- J. Kim, A.K. Bea, Y.H. Kim, D.W. Kim, K.Y. Lee, C.M. Lee, Improved suspension stability of calcium carbonate nanoparticles by surface modification with oleic acid and phospholipid, *Biotechnol. Bioprocess Eng.* 20 (2015) 794–799, <https://doi.org/10.1007/s12257-014-0898-3>.
- E. Fekete, B. Pukánsky, A. Toth, I. Bertoti, Surface modification and characterization of particulate mineral fillers, *J. Colloid Interface Sci.* 135 (1) (1995) 200–208, [https://doi.org/10.1016/0021-9797\(90\)90300-D](https://doi.org/10.1016/0021-9797(90)90300-D).
- V. Nikulshina, C. Gebald, A. Steinfeld,  $\text{CO}_2$  capture from atmospheric air via consecutive  $\text{CaO}$ -carbonation and  $\text{CaCO}_3$ -calcination cycles in a fluidized-bed solar reactor, *Chem. Eng. J.* 146 (2009) 244–248, <https://doi.org/10.1016/j.cej.2008.06.005>.
- G. Corro, N. Sánchez, U. Pal, F. Bañuelos, Biodiesel production from waste frying oil using waste animal bone and solar heat, *Waste Manag.* 47 (2016) 105–113, <https://doi.org/10.1016/j.wasman.2015.02.001>.
- G. Corro, U. Pal, N. Tellez, Biodiesel production from *Jatropha curcas* crude oil using  $\text{ZnO/SiO}_2$  photocatalyst for free fatty acids esterification, *Appl. Catal. B Environ.* 129 (2013) 39–47, <https://doi.org/10.1016/j.apcatb.2012.09.004>.
- Y. Zhang, M.A. Dube, D.D. McLean, Biodiesel production from waste cooking oil: 1. Process design and technological assessment, *Bioresour. Technol.* 89 (1) (2003) 1–16, [https://doi.org/10.1016/S0960-8524\(03\)00040-3](https://doi.org/10.1016/S0960-8524(03)00040-3).
- B. Engin, H. Demirtas, M. Eken, Temperature effects on egg shells investigated by XRD, IR and ESR techniques, *Radiat. Phys. Chem.* 75 (2006) 268–277, <https://doi.org/10.1016/j.radphyschem.2005.09.013>.
- C. Rodríguez-Navarro, E. Ruiz-Agudo, A. Luque, A.B. Rodríguez-Navarro, M. Ortega-Huertas, Thermal decomposition of calcite: mechanisms of formation and textural evolution of  $\text{CaO}$  nanocrystals, *Am. Mineral.* 94 (2009) 578–593, <https://doi.org/10.2138/am.2009.3021>.
- J. Lanás, J.I. Alvarez, Dolomitic limes: evolution of the slaking process under different conditions, *Thermochim. Acta* 423 (2004) 1, <https://doi.org/10.1016/j.tca.2004.04.016>.
- M. López-Granados, M.D. Zafra-Poves, D.M. Alonso, R. Mariscal, F. Cabello-Galisto, R. Moreno-Tost, J. Santamaría, J.L.G. Fierro, Biodiesel from sunflower oil using activated calcium oxide, *Appl. Catal. B.* 73 (2007) 317–326, <https://doi.org/10.1016/j.apcatb.2006.12.017>.

- [38] M. López Granados, D. Martín Alonso, I. Sádaba, R. Mariscal, P. Ocón, Leaching and homogeneous contribution in liquid phase reaction catalysed by solids: the case of triglycerides methanolysis using CaO, *Appl. Catal. B Environ.* 89 (2009) 265–272, <https://doi.org/10.1016/j.apcatb.2009.02.014>.
- [39] M. Brandao, E. Azzi, R.M.L. Novaes, A. Cowie, The modelling approach determines the carbon footprint of biofuels: the role of LCA in informing decision makers in government and industry, *Clean. Environ. Syst.* 2 (2021), 100027, <https://doi.org/10.1016/j.cesys.2021.100027>.
- [40] L.P. Christopher, H. Kumar, P. Zambare, Enzymatic biodiesel: challenges and opportunities, *Appl. Energy* 119 (2014) 497–520, <https://doi.org/10.1016/j.apenergy.2014.01.017>.